Research Article/ Mechanical Engineering, Mechatronics, and Materials Science https://doi.org/10.15446/ing.investig.v42n1.86698

Comparison of Treatments by Mercerization and Plasma Glow Discharge on Residues of the Amazon Chestnut Shell (*Bertholletia Excelsa*)

Comparación de tratamientos por mercerización y descarga intensa de plasma sobre residuos de la cáscara de castaña amazónica (*Bertholletia excelsa*)

Ximena Zapata-Londoño[1], James Janderson Rosero-Romo[2], Hugo Armando Estupiñán-Durán[3]

ABSTRACT

The chestnut shell from the Amazon region shared between Colombia, Brazil, and Perú is an abundant residue of the walnut used for obtaining food and cosmetic products. This residue is not yet usable due to the lack of knowledge of its properties and the environmental impact generated by its treatment through methods such as mercerization. This work presents the results of the characterization of Amazon chestnut shell residues treated by two methods, mercerization with NaOH solution and intense plasma discharge (Glow Discharge Plasma), in a reactor with argon gas in a 0,3-bar vacuum and discharge conditions of 80 mA and 600 s. The microstructural, morphological, topographic, and nanomechanical changes of the chestnut residues without treatment and with the two proposed treatments were evaluated by means of the μRaman, scanning electron microscopy, and atomic force microscopy techniques. The results showed the effectiveness of the plasma method over the mercerization method at obtaining more crystalline cellulose structures due to the reduction of hemicellulose, lignin, and the aqueous phase of walnut shell waste.

Keywords: Amazonian chestnut, *Bertholletia excelsa*, cellulose, plasma glow discharge

RESUMEN

La cáscara de castaña proveniente de la región amazónica, compartida entre Colombia, Brasil y Perú, es un residuo abundante de la nuez empleada en la obtención de productos alimenticios y cosméticos. Este residuo no es utilizable por la falta de conocimiento de sus propiedades y del impacto ambiental generado por su tratamiento por métodos como la mercerización. En este trabajo se muestran los resultados de la caracterización de los residuos de cáscara de castaña amazónica tratados por dos métodos, mercerización con solución de NaOH y descarga intensa de plasma (*Glow Discharge Plasma*), en un reactor con gas de argón en un vacío de 0,3 bar y condiciones de descarga de 80 mA y 600 s. Los cambios microestructurales, morfológicos, topográficos y nanomecánicos de los residuos de castaña sin tratamiento y con los dos tratamientos propuestos se evaluaron mediante las técnicas de μRaman, microscopía electrónica de barrido y microscopía de fuerza atómica. Los resultados mostraron la efectividad del método por plasma, por encima del método de mercerización, para la obtención de estructuras más cristalinas de celulosa debido a la reducción de la hemicelulosa, la lignina y la fase acuosa de los desechos de cáscara de nuez.

Palabras clave: castaña amazónica, *Bertholletia excelsa*, celulosa, descarga intensa de plasma

Received: April 27th, 2020
Accepted: May 4th, 2021

Introduction

Generating agricultural waste is inevitable, since a large amount of it can result from the harvest in the early stages of the food production chain, which causes environmental and economic problems in cultivation areas. Por example, one of the main economic activities in the Brazilian Amazon region is the Brazilian nut, whose shelling stage is a process that generates large amounts of waste, representing 90% by volume of the chestnut crops (Cardozo *et al.*, 2014; de Souza, E. S., *et al.*, 2019). This product is part of the so-called 'dried fruits', which provide important nutritional benefits due to their high content of proteins, carbohydrates, unsaturated lipids, essential vitamins, and minerals (ARS-US, 2019). However, Brazilian nut harvesting maintains a constant demand in the international market.

Bertholletia excelsa is the scientific name by which this walnut species is known, according to its taxonomy and ecology.

[1]Biological Engineering Student, Universidad Nacional de Colombia-Medellín, Colombia. Email: xzapatal@unal.edu.co
[2]Physical Engineer, Universidad Nacional de Colombia, Medellín, Colombia. M.Eng. in Engineering, Materials and processes, Universidad Nacional de Colombia, Medellín, Colombia. Email: jjroseror@unal.edu.co
[3]Metallurgical Engineer, Universidad Industrial de Santander, Colombia. M.Eng. in Engineering, Universidad Industrial de Santander, Colombia. Ph.D. in Chemical Engineering, Affiliation: Associate Professor, Universidad Nacional de Colombia, Medellín, Colombia. Email: haestupinand@unal.edu.co

How to cite: Zapata-Londoño, X., Rosero-Romo, J. J., and Estupiñán-Durán, H. A. (2022). Comparison of Treatments by Mercerization and Plasma Glow Discharge on Residues of the Amazon Chestnut Shell (*Bertholletia Excelsa*). *Ingeniería e Investigación*, *42*(1), e86698. 10.15446/ing.investig.v42n1.86698

It belongs to the *Lecythidaceae* family, found mainly in the Brazilian Amazon and several South American countries such as French Guyana, Suriname, Bolivia, Venezuela, Perú, and Colombia, due to the fact that its growth is favored by sandy or clayey soils with good drainage. Furthermore, it is an endemic species, and it is impossible to domesticate, since it forms a natural balance dependent on rodents and specific organisms for pollination (Melo *et al.*, 2018). Additionally, this species is representative of the Amazonian tropical forest, not only for its economic and environmental importance, but also for its size (up to 50 m), with a trunk that reaches 2 m in diameter (Salo *et al.*, 2013). Its fruit is extremely hard, with a shape similar to that of coconut, and it can weigh up to 2 kg with 12 to 25 nuts inside, each with its own shell (Bonelli *et al.*, 2001).

The Brazilian nut shell is mainly composed of cellulose, lignin, and hemicellulose, so a convenient option to reduce the impact of generating unusable waste would be using it as a source for obtaining fibrils and/or cellulose nanocrystals, which is especially important for the multiple applications it can have in the paper, textile, food, and nanotechnology industries, given its use in the manufacture of bio-nanocomposites, pharmaceuticals, biomedical implants, medicines, among others; it is classified as a non-toxic, highly crystalline, hydrophilic material with outstanding mechanical properties, especially due to its high rigidity. (Naduparambath *et al.*, 2018; de Souza, A. G. *et al.*, 2019).

To produce cellulose from biowaste, it is necessary to eliminate hemicellulose, lignin, and other components present in the lignocellulosic material that are rigidly associated through non-covalent bonds and covalent cross linkages (Tezcan and Atici, 2017). Figure 1 shows the molecular scheme of a lignocellulosic biomass, where hemicellulose is a carbohydrate polymer in the form of a network that covers the cellulose, and lignin is a polymer with an aromatic structure of a hydrophobic nature located between cellulose and hemicellulose fibers (Jagtap et al., 2018; Sun, *et al.*, 2016; Álvarez-Rodriguez *et al.*, 2012). Current methods for obtaining cellulose are based on delignifying, that is, eliminating lignin through chemical pretreatments such as acid hydrolysis, basic hydrolysis, high pressure steam, among others (de Souza E. S., *et al.*, 2019).

Basic hydrolysis is a very common method, also known as the 'mercerization method', used to remove lignin from plant fiber waste. During this process, lignin is generally reduced by means of diluted NaOH, causing the separation between the structural links of lignin and the carbohydrates found on the external surface of the biomass, given the increase in its internal surface area (swelling) (Jaramillo-Quiceno, 2016; Rosa *et al.*, 2010). One of the advantages of this method is the high efficiency in the solubilization of lignin. However, its treatment conditions imply the use of very expensive industrial equipment, as well as environmental and human health problems due to the use of chemical products (Tezcan and Atici, 2017).

Glow Discharge Plasma (GDP) is a new method for the surface treatment of materials. It is economic and friendly to the environment, and it allows transforming the surface properties and sometimes of the interior mass of metals, polymers, elastomers, ceramics, etc. Surface cleaning, etching, crosslinking, and changes in the chemical structure are some of the most important modifications reported in materials treated with this technique (Vacková *et al.*, 2019). Its operation consists of introducing a sample into a vacuum chamber under the action of a high-energy ionized gas (plasma) produced by an electric field within the chamber. The sample of interest interacts with cold ions, high-energy electrons, free radicals, and ultraviolet radiation, thus generating changes in their properties. These modifications depend on the working parameters of the plasma equipment: voltage, type of gas used, pressure, and the polarity of the sample versus the polarity of the equipment. In a polymer, for example, when the electrons collide with the surface, a break in the bonds and the formation of different molecular structures take place (Tsai *et al.*, 2010). Different industries all over the world are planning to incorporate the modification of the surface properties of many materials into their production lines. This includes textiles, polymeric fibers, food, packaging, and other materials of an inorganic and organic nature. Therefore, the study of the transformation of the properties of plant waste is a great opportunity to explore a wide range of interesting applications.

Studying the impact of technologies for the treatment of these new materials, specifically in the modification of vegetable fibers from agro-industrial waste, is one of the objectives of this research, as well as presenting the comparative results obtained from the treatment by intense plasma discharge and the treatment by mercerization of residues of chestnut walnut shell fibers, with respect to changes in morphology, microstructure, and mechanical behavior.

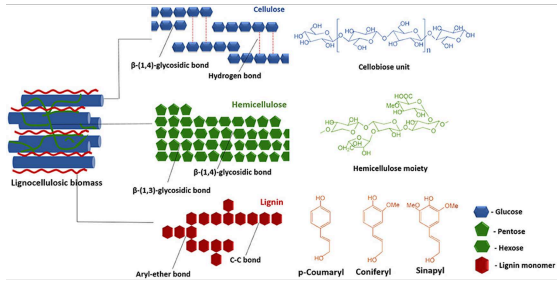

Figure 1. Molecular scheme of lignocellulosic biomass.
Source: Jagtap *et al.*, 2018

Experimental section

Materials and methods

The main objective of the methodological development proposed in this work was to prepare a useful residue extracted from the shell of the Amazonian chestnut using plasma glow discharge and mercerization treatments to compare the stiffness, morphological, topographic, and microstructural changes generated in the treated residues. To this effect, the collection and supply of seeds of the chestnut (*Bertholletia excelsa*) was carried out by residents of the jungle

near the city of Leticia, located in the Colombian Amazon region.

These seeds, approximately 4 to 5 cm in diameter, were washed with distilled water and simultaneously brushed to remove any adhering organic residue, before manually separating the shell and the fruit from the seed. This procedure was performed with a hammer, with extreme caution to avoid mixing the fruit of the walnut with the macerated shell. The residues obtained were reduced in size using a mortar and then separated by means of granulometric sieves with a 106-micron mesh, thus obtaining three triplicate samples of approximately 0,5 g each for study. A group of three of these samples was labeled as 'untreated', and the other two groups of three samples were marked as 'mercerized' and 'plasma', respectively.

For the mercerization process of the walnut shell residues, NaOH solution was used. The variables established as preliminary control were NaOH concentration, temperature, exposure time, and fiber weight to NaOH solution ratio. Then, in the main experimental phase, these variables were assumed to be constant, according to previous works (Jaramillo-Quiceno, 2016). For this, 0,5 g of sample were treated at a concentration of 4% NaOH, a temperature of 40 °C for 2 h, and a fiber: solution ratio of 1:15. After this step, the sample was washed and filtered with 1% acetic acid in solution and then rinsed with distilled water to remove unreacted NaOH residues and water-soluble extracts. After this alkaline treatment, the fibers were dried in two stages, the first for 24 hours at room temperature, and the second at 70 °C for 48 h in a drying oven to remove as much moisture as possible.

A Quorum Technologies Q150R sputtering reactor, adapted for the GDP process, was used on the crushed walnut shell samples, with an atmosphere of argon ionizing gas at a vacuum pressure of 0,3 bar and additional operating conditions of 80 mA, under positive polarity conditions in the sample holder and 600 s of processing time.

Raman spectra of the shell samples with and without their corresponding treatments were obtained with a LabRam HR Evolution Horiba Scientific micro-Raman-Confocal spectrometer coupled with an Olympus BX41 light microscope with a 100X objective for the qualitative analysis of chemical structures. To this effect, 0,15 g of each sample were manually compacted to eliminate dispersions and placed on a glass slide. Scans were performed in a range of 50 cm^{-1} to 3 500 cm^{-1} with a 785 nm laser and an acquisition time of 6 s with 12 accumulations. The software used to determine the bands of interest and the corresponding processing of the spectra obtained was LabSpace6, along with its database, while also processing the spectra acquired with the baseline and the univariate method with Lorentian adjustment, in order to obtain intensity values with greater precision.

Images were obtained from 500X to 2000X with a SEM EVO MA10 Carl Zeiss scanning electron microscope operating at a voltage of 5 kV and a working distance of 8,5 mm. This allowed analyzing and comparing the morphology of chestnut shell residues with and without the mercerization and plasma treatments. The observed samples were pre-coated with a thin layer of 5 nm gold (measured with a piezoelectric device conditioned in sputtering equipment), as is recommended for observing non-conductive samples in SEM.

Using the AFM Park Systems NX10 atomic force microscope in areas of 5 x 5 µm and 256 x 256 pixels, topography, dimensional distribution, and stiffness measurements of the treated and untreated chestnut shell residues were performed on the Pint Point scanning mode, with a tip on cantilever (reference NSC14 with a force constant of 5 N/m and a frequency of 160 KHz).

Results and discussion

The images of the untreated seeds and a scheme with the different stages of treatment are shown in Figure 2.

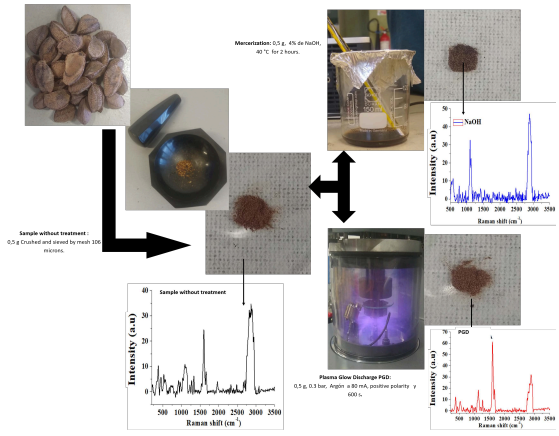

Figure 2. Chestnut husk treatments: a) Crushed and sieved, b) Mercerization, c) Plasma.
Source: Authors

The untreated chestnut shell shows a brown color, which manifests itself in the aqueous solution resulting from the mercerization treatment with NaOH due to a partial elimination of lignin (Rosa *et al.*, 2010). This color change did not occur in the chestnut shell samples treated with discharge plasma.

Crystallinity in cellulose has an important effect on the physical, mechanical, and chemical properties of the fibers and microfibers that constitute it. Similar works have found that a higher crystallinity increases tensile strength and gives greater dimensional stability and density to the fiber while decreasing properties such as chemical reactivity and swelling (Jaramillo-Quiceno, 2016; López-Durán *et al.*, 2018; Kathirselvam *et al.*, 2019). The Raman spectra of the fibers processed by mercerization and plasma, as well as of those unprocessed, are shown in Figures 3a, b, c, and d, where the variations in the intensity of the main bands represent, among other characteristics, changes in crystallinity and the reduction of lignocellulose from the residues of the Amazonian chestnut shell due to the treatments proposed in this research.

In Figure 3a, the predominant bands in the spectral region between 1 525 cm^{-1} and 1 700 cm^{-1} are presented, thus representing the aryl stretching vibration, which is symmetric

and mainly associated with lignin; as well as a 1 599 cm^{-1} band whose attenuation indicates the delignification of the fiber of shell residues from mercerization (Gierlinger *et al.*, 2013). In the Raman spectrum of plasma-treated fibers, the last band does not completely disappear; according to Segmehl *et al.* (2019), the typical distribution of lignin between hemicellulose and cellulose fibers is not uniform and, therefore, the location of the analyzed region is an important factor because there can be significant variations in the collected Raman signal. Taking this effect into account, the presented spectrum accounts for the average of several acquired. The bands of the spectra of the different analyzed samples located between 2 862 and 2 882 cm^{-1} represent the amorphous phase of cellulose, generally associated with the aqueous phase present in the residues. These bands decrease in intensity in the treated samples, mainly in the plasma-treated one. Table 1 shows the Raman band assignments for the Amazonian chestnut shell (*Bertholletia excelsa*).

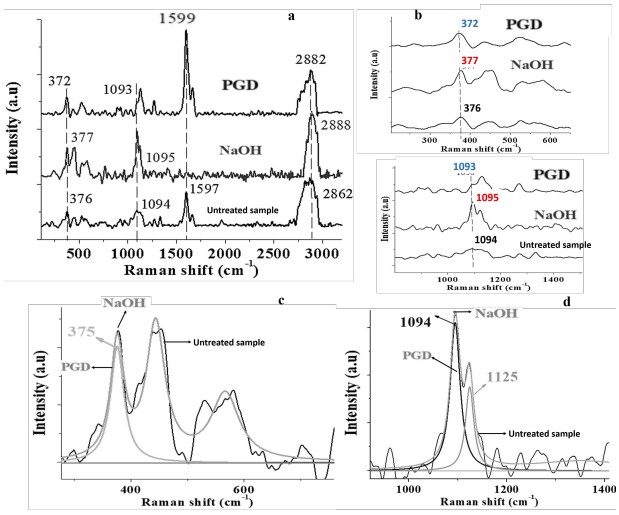

Figure 3. Raman spectra and Lorentzian adjustment: a) Raman spectra of chestnut fibers with and without mercerization and plasma treatments; b) Bands of interest for the analysis and adjustment to calculate the percentage of crystallinity; c-d) Lorentzian adjustment for bands 375 cm^{-1} and 1 094 cm^{-1}.
Source: Authors

Figure 3b shows the bands of the Raman spectra representing the loss of cellulose in the untreated walnut shell fibers at 374 and 1 096 cm^{-1}, those treated by mercerization at 377 and 1 095 cm^{-1}, and those plasma-treated at 372 and 1 093 cm^{-1}. Figures 3c and d show spectra with these bands of interest with a Lorentzian-type fit. In Figure 3b, the Raman bands between 1 096 and 1 122 cm^{-1} are associated with the stretching of the typical glycosidic bond of cellulose. The spectra with Lorentzian analysis in Figure 3d show the definition of the bands at 1 094, 1 095, and 1 125 cm^{-1}, which represent partial and non-total loss of cellulose after the mercerization and plasma treatments. The transformation from type I to type II cellulose is generally related to the variation of the band at 380 cm^{-1}, according to studies carried out on fibers treated by mercerization with NaOH (Segmehl *et al.*, 2019). However, in this study, the position of this band for the three cases, 376, 377, and 372 cm^{-1} is relatively similar, although modifications to the bandwidth are observed due to the defects induced from the treatments on the walnut shell fibers.

Table 1. Raman band assignments for Amazonian chestnut shell (*Bertholletia excelsa*) samples

Chemical species	Raman Shift (cm^{-1})	Band assignment
Lignin	1 599, 1 597	Aryl ring stretching, symmetric
Cellulose	372, 377, 376	β-D-glucosides
	1 093, 1 095, 1 094	C-O-C stretching, asymmetric
	1 122, 1 125	C-O-C stretching, asymmetric
Hemicellulose	2 882, 2 888, 2 862	C-H stretching

Source: Authors

Considering that the changes in cellulose crystallinity are attributed to the degradation of lignocellulose and hemicellulose, a method has been proposed to quantitatively determine these changes based on the ratio of the intensities of the bands at 380 and 1 096 cm^{-1} (I_{380}/I_{1096}) and a data treatment with univariate analysis to solve problems involving the presence of fluorescence in the spectra (Agarwal *et al.*, 2010; Agarwal *et al.*, 2013). Similar works to determine the crystallinity of cellulose fibers have used X-ray diffraction patterns, with discrepancies in the reliability of the results obtained when varying the size of the fibers (Carrión-Prieto *et al.*, 2019). Contrary to the spectra obtained in this study, due to the interaction of the signal that relates hemicellulose and pectin, a Raman dispersion can be produced, leading to an imprecise measurement of cellulose crystallinity (Anderson *et al.*, 2003). According to this method, to determine the percentage of crystallinity in the walnut shell cellulose fibers, four Raman spectra have been processed for each treatment for their respective calibration, thus obtaining values of I_{375}/I_{1094}. In this sense, Equation (1) has been used to obtain the percentage of crystallinity (X_{Raman}) of the samples not treated and treated by GDP and mercerization.

$$X_{Raman} = \frac{\left(\frac{I_{375}}{I_{1094}}\right) - 0{,}0375}{0{,}0214} \times 100 \qquad (1)$$

The results of this analysis are presented in Table 2.

According to Table 2, the 1,5 value of I_{375}/I_{1094} reported for the sample treated by GDP (I_{372}/I_{1095}) represents the highest value of cellulose crystallinity with respect to the values of 0,62 and 0,94 reported for the samples treated by mercerization and without treatment, respectively. The presence of the Raman spectral band at 1 599 cm^{-1} corresponding to the structural vibration of lignocellulose in untreated and plasma-treated walnut shell microfibers, which does not appear in the sample treated by mercerization, affects the value of the intensity of the band at 1 094 cm^{-1}, whose value is higher in the sample treated by mercerization. Figure 4 shows the calibration graph of the four spectra taken in each sample, as well as the graph that relates the percentages of crystallinity vs. the calculated I_{375}/I_{1094} ratio.

Table 2. Raman intensity values and I_{375}/I_{1094} ratio for the calculation of the X_{Raman} crystallinity factor

SAMPLE	Raman Shift (cm^{-1})	Intensity (a.u)	I_{375}/I_{1094}	X_{Raman} (%)
Treated with NaOH	377, 1 095	20, 32	0,62	27,82
Treated with GDP	372, 1 095	12, 8	1,5	63,71
Without treatment	376, 1 093	10, 25	0,94	42,55

Source: Authors

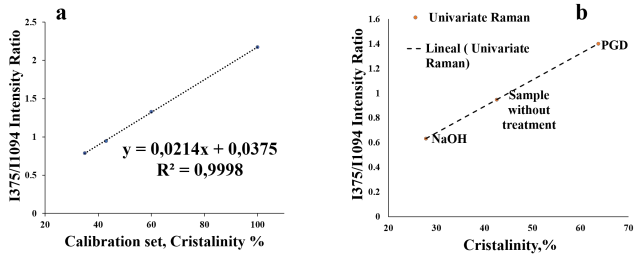

Figure 4. a) Graph showing the relationship between the crystallinity of the calibration set versus the Raman intensity ratio I_{375}/I_{1094}; b) Graph that relates the crystallinity of each sample with the Raman intensities I_{375}/I_{1094} with univariate analysis.
Source: Authors

According to the graph in Figure 4b, shown in ascending order by the degree of crystallinity, the walnut shell fibers treated by mercerization had a value of 27%, 42% for the sample without treatment, and 64% for the fiber treated by GDP. These values, as well as the I_{375}/I_{1094} ratio, probably show some dispersion due to the presence of lignocellulose, which especially affects the band associated with microcrystalline cellulose at 1 095 cm^{-1}. This band has been used for the study of mechanical properties in vegetable fibers, specifically for changes in viscoelastic properties (Eichhorn and Young, 2001).

Morphological description of the fibers by Scanning Electron Microscopy (SEM)

Figure 5 shows the SEM images of the fibers with and without the treatments. The surfaces of the shell residues have rough and porous shapes, thus evidencing the presence of amorphous regions associated with morphologies other than cellulose, such as lignin and hemicellulose (Figure 5a and b). In the fibers treated by that mercerization and GDP, the size of the cellulose microfibers was identified between 1,5 and 2,5 µm.

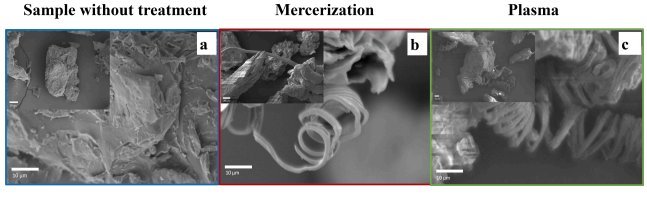

Figure 5. Morphological analysis: a) Image of the sample without treatment; b) Chestnut husk fibers with mercerization treatment in NaOH; c) Chestnut fibers with 80 mA plasma treatment.
Source: Authors

Likewise, Rosa *et al.* (2010), in their research on coconut shells, related what was observed in SEM images with the partial removal of impurities (lignin, hemicellulose, and other compounds present in the shell) based on partial fibrillation, unlike the untreated sample. Results obtained by the µRaman Spectroscopy technique of the plasma-treated samples are characterized by the presence of bands associated with cellulose, which are more defined than the bands of the samples without treatment. However, in both the mercerization and plasma treatment, they showed a level of partial defibrillation with a still compact morphology, similar to the morphology of the samples without treatment (according to the comparison in Figure 5a, b, and c), thus corroborating the results showing the Raman bands associated with lignin. In addition to this comparative analysis, it should be noted that the chestnut walnut shell sample with the highest defibrillation was the plasma-treated one, where long, continuous, spirally wound shapes of fibers of approximately 2,5 µm of diameter were observed.

Atomic Force Microscope (AFM)

Figure 6a shows the topographic characteristics of a walnut shell sample without any treatment, and Figures 6b and c, the topography images of the samples treated by mercerization and plasma, respectively. From this characterization, roughness measurements in Ra (µm) were obtained, observing a decrease in in this value for the samples treated by mercerization and by plasma in their order.

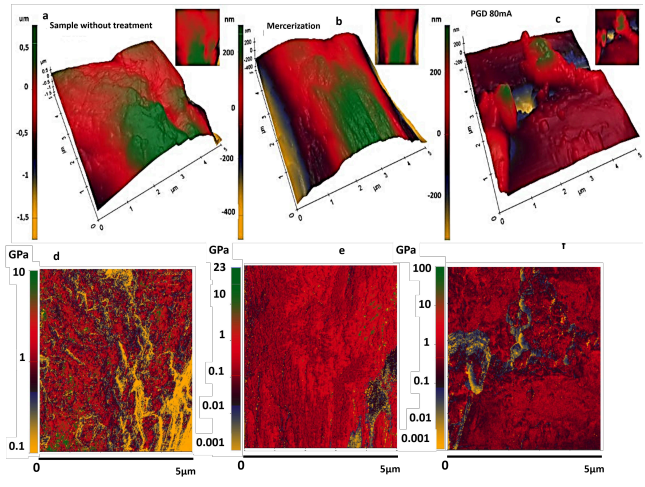

Figure 6. AFM images of topography (3D) and stiffness (2D): a) untreated sample topography, b) mercerization-treated sample topography, c) plasma-treated sample topography, d) Stiffness image for untreated sample, e) Stiffness image for sample treated by mercerization, f) Stiffness image for sample treated by plasma.
Source: Authors

This aspect is associated with the effect of mercerization and plasma treatment on the removal of cementitious material from the walnut shell or the structure of its first amorphous region, which is mainly composed of hemicellulose and lignin, which corroborates the results obtained through Raman and SEM imaging. The decrease in the roughness of the surfaces

of the walnut shells after plasma treatment is caused by the breakdown of the amorphous structures of hemicellulose and lignin that are present in the primary layer of microfibrils, thus exposing a secondary layer rich in cellulose crystalline and with a smooth topography. Table 3 shows the values of roughness Ra (μm) and stiffness (GPa) obtained.

Table 3. Roughness Ra (μm) and Stiffness (GPa) values for chestnut nut fibers without treatment and with treatment

SAMPLE	Ra (μm)	Stiffness (GPa)
Treated with NaOH	0,137 ± 0,013	11,55 ± 0,2
Treated with GDP	0,071 ± 0,01	88,4 ± 0,2
Without treatment	0,193 ± 0,010	5,94 ± 0,3

Source: Authors

Figures 6d, e, and f refer to the images acquired by the AFM's Pin-Point mode, showing the variation of the stiffness on the surface (5 x 5 μm) of the walnut shell residues. In the gray bar, the different color tones ranging from light gray, medium light gray, medium dark gray, and dark gray indicate the variation of stiffness in the range of 0,001 to 100 GPa. Medium dark gray and dark gray represent the areas with the highest stiffness distribution in the walnut shell residues and the most representative of the physical-mechanical changes manifested from the treatments developed in this research. In the untreated walnut shell samples, this zone appears between 0,7 and 7 GPa, with the notable presence of less rigid zones (between 0,1 and 0,7 GPa) in a light gray color tone. In Figure 6e (a sample treated by mercerization), the stiffer zones appear between 0,05 and 8 GPa, with a small distribution of less rigid structures between 0,001 and 0,3 GPa (light gray color tone). For the plasma-treated walnut shell sample shown in Figure 6f, values between 0,09 and 35 GPa represent areas of higher rigidity, and those between 0,001 and 0,09 GPa correspond to less rigid areas.

Treatment processes in vegetable fibers, especially mercerization, generally produce lignin and hemicellulose removal effects on the fibers (Cheng and Wang, 2008; Cousins, 1978). While comparing the stiffness results of the different treated and untreated walnut shell samples, it was observed that the most notable changes occurred in the GDP-treated samples. From the process by plasma in vegetable fibers, it is known that the decrease in cellulose, hemicellulose, and lignin is caused by the breakdown of the glucoside bonds of cellulose, of the sugars present in the structure of hemicellulose, and the carboxylic and hydroxyls bonds in cellulose, thus generating a molecular restructuring of the carbon covalent bonds of the fibers with respect to oxygen ions. This causes important changes in the stiffness of the treated structures. Several studies have reported that the increase in stiffness is associated with a more crystalline structuring of cellulose microfibrils, which is consistent with the results obtained by AFM imaging, the morphological and structural changes observed in the SEM characterization, and the analysis of the spectral bands obtained by Raman (Marcuello *et al.*, 2019).

In the third column of Table 3, the stiffness values obtained by analysis in the AFM XEI software are shown. This procedure consists of processing the images acquired and shown in Figure 6d-f to obtain an arithmetic average in GPa of the selected region. A higher average stiffness value was found in the plasma-treated samples, which matches the values analyzed in the gray tone bands of their respective images. An important aspect to consider when processing the fibers with plasma is the drastic decrease in the humidity of the fibers due to the vacuum of the procedure. This reduces their viscoelastic properties, with the obvious consequence of increasing the rigidity of the walnut shell. This behavior was also observed in the samples treated by mercerization, which presented a stiffness value of twice that of the samples without treatment and almost eight times less than that of the samples treated with plasma. In general terms, the increase in the level of crystallinity and the stiffness of the walnut shell fibers is a consequence of the covalent molecular restructuring of the carbon and oxygen bonds of the fibers, in addition to the decrease in the aqueous phase (Marcuello *et al.*, 2019).

Conclusions

Both the mercerization and plasma treatment on the Amazonian chestnut walnut shell generated the release of agglomerated cellulose microfibers in spirals with diameters between 1,5 and 2,5 μm, according to the SEM image analysis. The Raman spectra for both treatments used in this research showed bands associated with the presence of cellulose, with the disappearance of the 1 599 cm^{-1} band related to lignin degradation, with a greater effect in the treatment by mercerization than by plasma.

Additionally, the calculation of the crystallinity index proposed in this work with the relation of intensities associated with cellulose showed a significant increase in crystallinity for plasma-treated samples compared to the untreated samples, as well as a decrease in crystallinity in the sample treated by mercerization, which indicates a transformation effect based on the breakdown and covalent restructuring of carbon-oxygen bonds in the fibers treated by plasma, and a structural breakdown effect with a low level of reconstitution for the mercerization treatment.

In addition to this, the plasma treatment decreased the aqueous phase associated with cellulose, hemicellulose, and amorphous lignin, thus affecting the original viscoelastic properties of the chestnut shell residues and increasing their rigidity, as evidenced in the results obtained by AFM on the Pin-Point itinerant contact mode. However, an important effect must be added to the increase in the rigidity of the shell, based on the restructuring of the carbon-oxygen bonds that occurs after the removal of the first amorphous wall of hemicellulose and lignin, which exposes a second wall composed of crystalline cellulose, partially free of these amorphous substructures. This was an important factor for the decrease in the roughness of the structure treated by plasma.

References

Agarwal, U., Reiner, R. S., and Ralph, S. A. (2010). Cellulose I crystallinity determination using FT–Raman spectroscopy: univariate and multivariate methods. *Cellulose, 17,* 721-733. 10.1007/s10570-010-9420-z

Agarwal, U. P., Reiner, R. R., Ralph, S. A., Forest, A., Gi, O., and Drive, P. (2013). Estimation of Cellulose Crystallinity of Lignocelluloses Using Near-IR. *Journal of Agricultural and Food Chemistry, 61*,103-113. 10.1021/jf304465k

Bonelli, P., Della Rocca, P., Cerrella, E., and Cukierman, A. (2001). Effect of pyrolysis temperature on composition, surface propeties and thermal degradation rates of Brazil Nut shells. *Bioresource Technology*, *76*(1), 15-22. 10.1016/S0960-8524(00)00085-7

Álvarez Rodriguez, A., Pizarro-Garcia, C., and Folgueras-Díaz, M.-B. (2012). Caracterización química de biomasa y su relación con el poder calorífico. *Repositorio Institucional de La Universidad de Oviedo*, 1-12. https://digibuo.uniovi.es/dspace/bitstream/handle/10651/17777/TFM_Ana_AlvarezProteg.pdf;jsessionid=61CEC16628EFBE55B4399447CD243E32?sequence=6

Cardozo, E., Erlich, C., Alejo, L., and Fransson, T. H. (2014). Combustion of agricultural residues: An experimental study for small-scale applications. *Fuel, 115*, 778-787. 10.1016/J.FUEL.2013.07.054

Cheng, Q. and Wang, S. (2008). A method for testing the elastic modulus of single cellulose fibrils via atomic force microscopy. *Composites Part A, 39*(12), 1838-1843. 10.1016/j.compositesa.2008.09.007

Cousins, W. J. (1978). Young's modulus of hemicellulose as related to moisture content. *Wood Science and Technology, 12*(3), 161-167. 10.1007/BF00372862

Eichhorn, S. J. and Young, R. J. (2001). The Young's modulus of a microcrystalline cellulose. *Cellulose, 8,* 197-207. 10.1023/A:1013181804540

Hepworth, D. and Bruce, D. (2000). The Mechanical Properties of a Composite Manufactured from Non-Fibrous Vegetable Tissue and PVA. *Composites Part A: Applied Science and Manufacturing, 31*(3). 283-285. 10.1016/S1359-835X(99)00100-1

Gierlinger, N., Keplinger, T., Harrington, M., and Schwanninger, M. (2013). *Raman Imaging of Lignocellulosic Feedstock*. IntechOpen. 10.5772/50878

Baruah, J., Nath, B. K., Sharma, R., Kumar, S., Deka, R. C., Baruah, D. C., and Kalita, E. (2018). Recent Trends in the Pretreatment of Lignocellulosic Biomass for Value-Added Products. *Frontiers in Energy Research, 6*, 141. 10.3389/fenrg.2018.00141

Jaramillo-Quiceno, N. (2016). *Efecto del proceso de mercerización en el comportamiento de la fibra de hoja de piña (FHP) como refuerzo en una matriz de polipropileno*. https://www.semanticscholar.org/paper/Efecto-del-proceso-de-mercerizaci%C3%B3n-en-el-de-la-de-Quiceno/13945ae8739e1372c068a89d71cd96e6d9a896ac

Kathirselvam, M., Kumaravel, A., Arthanarieswaran, V. P., and Saravanakumar, S. S. (2019). Isolation and characterization of cellulose fibers from *Thespesia populnea* barks: A study on physicochemical and structural properties. *International Journal of Biological Macromolecules, 129*, 396-406. 10.1016/j.ijbiomac.2019.02.044

López-Durán, V., Larsson, P. A., and Wågberg, L. (2018). Chemical modification of cellulose-rich fibres to clarify the influence of the chemical structure on the physical and mechanical properties of cellulose fibres and thereof made sheets. *Carbohydrate Polymers, 182*, 1-7. 10.1016/j.carbpol.2017.11.006

Marcuello, C., Foulon, L., Chabbert, B., Aguié-béghin, V., and Molinari, M. (2019). Young's modulus of lignocellulosic polymers and their adhesion with. *International Journal of Biological Macromolecules, 147*, 1064-1075. 10.1016/j.ijbiomac.2019.10.074

Melo, V. F., Batista, A. H., Barbosa, J. Z., Barbeiro, L., Gomes, R., and Dultra, M. T. M. (2018). Soil quality and reforestation of the Brazil nut tree (*Bertholletia excelsa* Bonpl.) after laterite-type bauxite mining in the Brazilian Amazon forest. *Ecological Engineering, 125*, 111-118. 10.1016/j.ecoleng.2018.10.016

Naduparambath, S., Jinitha, T. V., Shaniba, V., Serejith, M. P., Balan, A. K., and Purushothaman, E. (2018). Isolation and characterization of cellulose nanocrystals from sago seed shells. *Carbohydrate Polymers, 180*, 13-20. 10.1016/J.CARBPOL.2017.09.088

Carrión-Prieto, P., Martín-Ramos, P. Hernández-Navarro, S., Sánchez-Sastre, L. F., Marcos-Robles, J. L., and Martín-Gil, J. (2019). Crystallinity of cellulose microfibers derived from *Cistus ladanifer* and *Erica arborea* shrubs. *Maderas. Ciencia y tecnología, 21*(4), 447-456. 10.4067/S0718-221X2019005000402

Rodriguez-Álvarez, A., Pizarro, C., and Folgueras, M. (2012). Caracterización Química De Biomasa Y Su Relación. *Universidad de Oviedo*. https://digibuo.uniovi.es/dspace/bitstream/handle/10651/17777/TFM_Ana_AlvarezProteg.pdf;jsessionid=61CEC16628EFBE55B4399447CD243E32?sequence=6

Rosa, M. F., Medeiros, E. S., Malmonge, J. A., Gregorski, K. S., Wood, D. F., Mattoso, L. H. C., Glenn, G., Orts, W. J., and Imam, S. H. (2010). Cellulose nanowhiskers from coconut husk fibers: Effect of preparation conditions on their thermal and morphological behavior. *Carbohydrate Polymers*, *81*(1), 83-92. 10.1016/j.carbpol.2010.01.059

Salo, M., Sirén, A., and Kalliola, R. (2013). Collect Locally, Eat Globally – The Journey of the Brazil nut. *Diagnosing Wild Species Harvest, 2013*, 143-160. 10.1016/B978-0-12-397204-0.00008-5

Segmehl, J. S., Keplinger, T., Krasnobaev, A., Berg, J. K., Willa, C., and Burgert, I. (2019). Facilitated delignification in CAD deficient transgenic poplar studied by confocal Raman spectroscopy imaging. *Spectrochimica Acta Part A: Molecular and Biomolecular Spectroscopy, 206*, 177-184. 10.1016/j.saa.2018.07.080

de Souza, A. G., Rocha, D. B., Kano, F. S., and Rosa, D. d. S. (2019). Valorization of industrial paper waste by isolating cellulose nanostructures with different pretreatment methods. *Resources, Conservation and Recycling, 143*, 133-142. 10.1016/J.RESCONREC.2018.12.031

de Souza, E. S., Dias, Y. N., da Costa, H. S. C., Pinto, D. A., de Oliveira, D. M., de Souza Falção, N. P., Texeira, R. A., and Fernandes, A. R. (2019). Organic residues and biochar to immobilize potentially toxic elements in soil from a gold mine in the Amazon. *Ecotoxicology and Environmental Safety*, *169*, 425-434. 10.1016/J.ECOENV.2018.11.032

Sun, S., Sun, S., Cao, X., and Sun, R. (2016 delete that). The role of pretreatment in improving the enzymatic hydrolysis of lignocellulosic materials. *Bioresource Technology, 199*, 49-58. 10.1016/j.biortech.2015.08.061

Tezcan, E. and Atici, O. G. (2017). A new method for recovery of cellulose from lignocellulosic bio-waste: Pile processing. *Waste Management*, *70*, 181-188. 10.1016/J.WASMAN.2017.09.017

Tsai, G., Montero, J., Calle, W., Quinde, M., and Sarmiento, P. (2010). Plasma: una tecnología de gran potencial para la industria y la ciencia. *Ingenius, 4*, 66-72. 10.17163/ings.n4.2010.07

U.S. Department of Agriculture (2010). *National Nutrient Database for Standard Reference, Food, nut and seed products Group: 12*. https://fdc.nal.usda.gov/ndb/search/list%20United

U.S. Department of Agriculture, Agricultural Research Service (ARS-US) (2019). *Food Data Central*. https://fdc.nal.usda.gov

Vacková, T., Špatenka, P., and Balakrishna, S. (2019). Plasma Treatment of Powders and Fibers. In Thomas, S., Mozetič, M., Cvelbar, U., Špatenka, P., and Praveen, K. M. (Eds.) *Non-Thermal Plasma Technology for Polymeric Materials* (pp. 193-210). Elsevier. 10.1016/b978-0-12-813152-7.00007-x